nature climate change

SUPPLEMENTARY INFORMATION

DOI: 10.1038/NCLIMATE2903

Power-generation system vulnerability and adaptation to changes in climate and water resources

Michelle T.H. van Vliet[1,2,*], David Wiberg[2], Sylvain Leduc[2], Keywan Riahi[2]

[1] Earth System Science, Wageningen University, PO Box 47, 6700 AA Wageningen, The Netherlands

[2] International Institute for Applied Systems Analysis (IIASA), Schlossplatz 1, A-2361 Laxenburg, Austria

* e-mail corresponding author: michelle.vanvliet@wur.nl

1) Global hydrological-electricity modelling framework

We developed a coupled hydrological-electricity modelling framework consisting of a hydrological model, stream temperature model, hydropower and thermoelectric power models. The hydrological component consists of the Variable Infiltration Capacity (VIC) model[1], which is a grid-based macro-scale hydrological model that solves both the surface energy and water balance. The VIC model was applied using the elevation, vegetation and soil characteristics as described in Nijsen et al.[2], which was later implemented at 0.5°x0.5° and using the DDM30 routing network[3] for lateral routing of streamflow. The reservoir scheme of Haddeland et al.[4] which is combined with an offline routing model[5] was used to obtain a more realistic representation of streamflow below reservoirs. Reservoir operations are assumed to follow simple operational rules based on the purpose(s) of dams. An optimization scheme based on the SCEM-UA algorithm[6] was used to calculate optimal releases using reservoir inflow, storage capacity and downstream water or power demands, as described by Haddeland et al[4]. The reservoir scheme uses a single-reservoir algorithm and does not consider the simultaneous operation of multiple reservoirs in a river basin. The economic value of reservoir releases for hydropower and water supply was assumed to be constant throughout the year, because of a lack of detailed information of this for dams on a worldwide level. At the beginning of each operational year the inflows for the next twelve months were used to determine reservoir releases. The reservoir scheme is intended for use in large-scale hydrologic modelling and implies lower performance than for a detailed reservoir model that utilizes site specific operating rules[4]. Nevertheless, this reservoir scheme has previously been successfully applied for continental[4,7] and global-scale scenario studies[8] and in regions where reservoir operation information and physical data are limited[9].

The water temperature component of our modelling framework consist of the process-based stream temperature model RBM, which solves the 1D-heat advection equation using a mixed Eulerian-Lagrangian approach[10,11]. RBM was modified for global-scale application including anthropogenic impacts (i.e. heat effluents and reservoir impacts) on water temperature[12,13]. Impacts of anthropogenic heat effluents from thermoelectric power plants on water temperature were incorporated by representing thermal discharges as point sources in the heat-advection equation (see supplementary information of van Vliet et al.[13] for details). For the assessment of return flow temperatures of thermal effluents we assumed that the temperature of the return flow is on average 3°C higher than the inlet river temperatures as described by van Vliet et al[13]. The headwater temperatures (boundary conditions) were estimated using the nonlinear water temperature regression model of Mohseni et al[14].

The main uncertainties related to the structure and parameterization of the VIC hydrological model and the stream temperature model RBM are assessed in previous work[11,12,15]. These studies showed that uncertainties are mainly attributed to the parametrization of soil and land cover (vegetation characteristics), heterogeneity in hydraulic characteristics and estimated boundary conditions (head water temperatures). For more details about the hydrological and stream temperature model, uncertainties and application to river basins worldwide we refer to van Vliet et al[12].

For the global electricity modelling part of our framework, we selected hydropower and thermoelectric power models that are suitable to quantify the physical impacts of changes in water resources on usable power plant capacity under climate change. Economic feedbacks of the assessed water constraints and related adaptation options (e.g. on energy prices, supply-demands portfolio) are not modelled in this study.

Hydropower usable capacity was quantified using the following equation.

$$P_{hydro} = Q \cdot H \cdot \rho_w \cdot g \cdot \eta \qquad (1)$$

Where: P_{hydro} = usable capacity of hydropower plant [W]; Q = streamflow [m^3/s]; H = hydraulic head [m]; ρ_w = density fresh water [kg/m^3]; g = gravitational acceleration [m/s^2]; η = total efficiency.

Thermoelectric power usable capacity was quantified for plants extracting river water for cooling by using the model of Koch and Vögele[16], which was modified as described in van Vliet et al[13]. This model simulates the required water demand for cooling and then the usable power plant capacity based on required water withdrawal, streamflow, water temperature and power plant specific characteristics (e.g. efficiency (depending on technology), cooling system type, environmental restrictions on maximum temperatures and maximum extractions of river water for cooling). The model makes a distinction between thermoelectric power plants using once-through cooling (equation 2) and recirculation (wet tower) cooling (equation 3).

Once-through cooling systems:

$$q = KW \cdot \frac{1-\eta_{total}}{\eta_{elec}} \cdot \frac{(1-\alpha)}{\rho_w \cdot C_p \cdot \max(\min((Tl_{\max} - Tw), \Delta Tl_{\max}), 0)} \qquad (2a)$$

$$P_{thermo} = \frac{\min((\gamma \cdot Q), q) \cdot \rho_w \cdot C_p \cdot \max(\min((Tl_{\max} - Tw), \Delta Tl_{\max}), 0)}{\frac{1-\eta_{total}}{\eta_{elec}} \cdot \lambda \cdot (1-\alpha)} \qquad (2b)$$

Recirculation (wet tower) cooling systems:

$$q = KW \cdot \frac{1-\eta_{total}}{\eta_{elec}} \cdot \frac{(1-\alpha) \cdot (1-\beta) \cdot \omega \cdot EZ}{\rho_w \cdot C_p \cdot \max(\min((Tl_{\max} - Tw), \Delta Tl_{\max}), 0)} \qquad (3a)$$

$$P_{thermo} = \frac{\min((\gamma \cdot Q), q) \cdot \rho_w \cdot C_p \cdot \max(\min((Tl_{\max} - Tw), \Delta Tl_{\max}), 0)}{\frac{1-\eta_{total}}{\eta_{elec}} \cdot \lambda \cdot (1-\alpha) \cdot (1-\beta) \cdot \omega \cdot EZ} \qquad (3b)$$

Where: q = daily cooling water demand [$m^3 s^{-1}$]; P_{thermo} = usable capacity of thermoelectric power plant [MW]; KW = installed capacity of thermoelectric power plant [MW]; η_{total} = total efficiency [%]; η_{elec} = electric efficiency [%]; α = share of waste heat not discharged by cooling water [%]; β = share of waste heat released into the air; ω: correction factor accounting for effects of changes in air temperature and humidity within a year; EZ = densification factor accounting for replacement of water in cooling towers to avoid high salinity levels; λ = correction factor accounting for the effects of reductions in efficiencies when power plants are operating at low capacities; ρ_w = density fresh water [kg m^{-3}]; C_p = heat capacity of water [J kg^{-1} $°C^{-1}$]; Tl_{max} = maximum permissible temperature of the cooling water [°C]; ΔTl_{max} = maximum permissible temperature increase of the cooling water [°C]; γ = maximum fraction of streamflow to be withdrawn for cooling of thermoelectric power plants [%]; Tw = daily mean river temperature [°C]; Q = daily streamflow [$m^3 s^{-1}$].

For power plants with combination cooling systems (once-through cooling with a supplementary cooling tower), we used the equations for recirculation (tower) cooling systems with parameter values representing the combined conditions of once-through and tower cooling. Differences in fuel sources (e.g. coal, oil, gas, nuclear, biomass) in the model are included by different efficiency values. For each power plant, we calculated daily q and

P_{thermo} using the daily streamflow and water temperature simulations for the grid cell where the power plant is located. To estimate λ we calculated the ratio of the usable capacity to installed capacity. When the ratio of usable capacity to installed capacity decreased to <50% (strong impacts of constraints), λ was reduced from 1 to 0.9 (with 10%) to simulate the extra efficiency loss under these conditions of power plant operation at low capacity.

2) Characteristics of hydropower and thermoelectric power plants worldwide

Both the hydropower and thermoelectric power models were applied on plant individual level. We extracted daily simulated streamflow and water temperature for the grid cell in which each power plant is situated. Impacts of changing streamflow and water temperature under climate change on usable capacity were quantified for 24,515 hydropower plants and 1,427 thermoelectric power plants worldwide. Information of power plant characteristics was obtained from the World Electric Power Plant Database (WEPPD) version 2013 [17]. The exact location of power plants is not included in this database. Therefore, latitude and longitude were estimated by linking the plant names of the power plants from WEPPD to the plant names of the Carbon Monitoring for Action database[18] in combination with the settlements points from the Socioeconomic Data and Applications Center database[19].

Our study focusses on conventional hydropower plants and for thermoelectric power we selected plants based on the following criteria: availability of information on cooling system type, source of fuel and installed capacity, and use of river water as the source for cooling. Information on cooling system type was reported by WEPPD for only a selection of thermoelectric power plants (38%). Based on all thermoelectric power plants for which the cooling system is reported we found that 7.9% use dry (air) cooling, 21.9% use sea water cooling and the remaining 70.2% use fresh water resources for cooling. For the power plants using freshwater, the largest part (95.5%) uses river water and a small part uses cooling lakes or ponds (4.1%) or groundwater (0.4%). In our study we focused on 1,427 thermoelectric power plants using river water for cooling and these account for 67.0% of the thermoelectric power plants for which cooling system type is reported in WEPPD. These thermoelectric power plants together contribute 28% of the total thermoelectric power installed capacity as reported by EIA[20]. The spatial (geographic) distribution of the selected thermoelectric power plants over continents is comparable with the distribution of all thermoelectric power plants from WEPPD (see Fig S1a). There are no indications that the 1,427 selected thermoelectric power plants are located in regions with stronger impacts of climate change and changes in streamflow (Fig S1b) and water temperature (Fig S1c) than the full dataset of 80,789 thermoelectric power plants of WEPPD for which latitude and longitude were estimated. Also the distribution of years that thermoelectric plants went in commercial operation (age distribution) for the selected 1,427 thermoelectric power plants is comparable with the full dataset of thermoelectric power plants from WEPPD (Fig S1d). We therefore consider this selection as representative for studying the impacts of climate change and changes in water resources on thermoelectric power usable capacity worldwide.

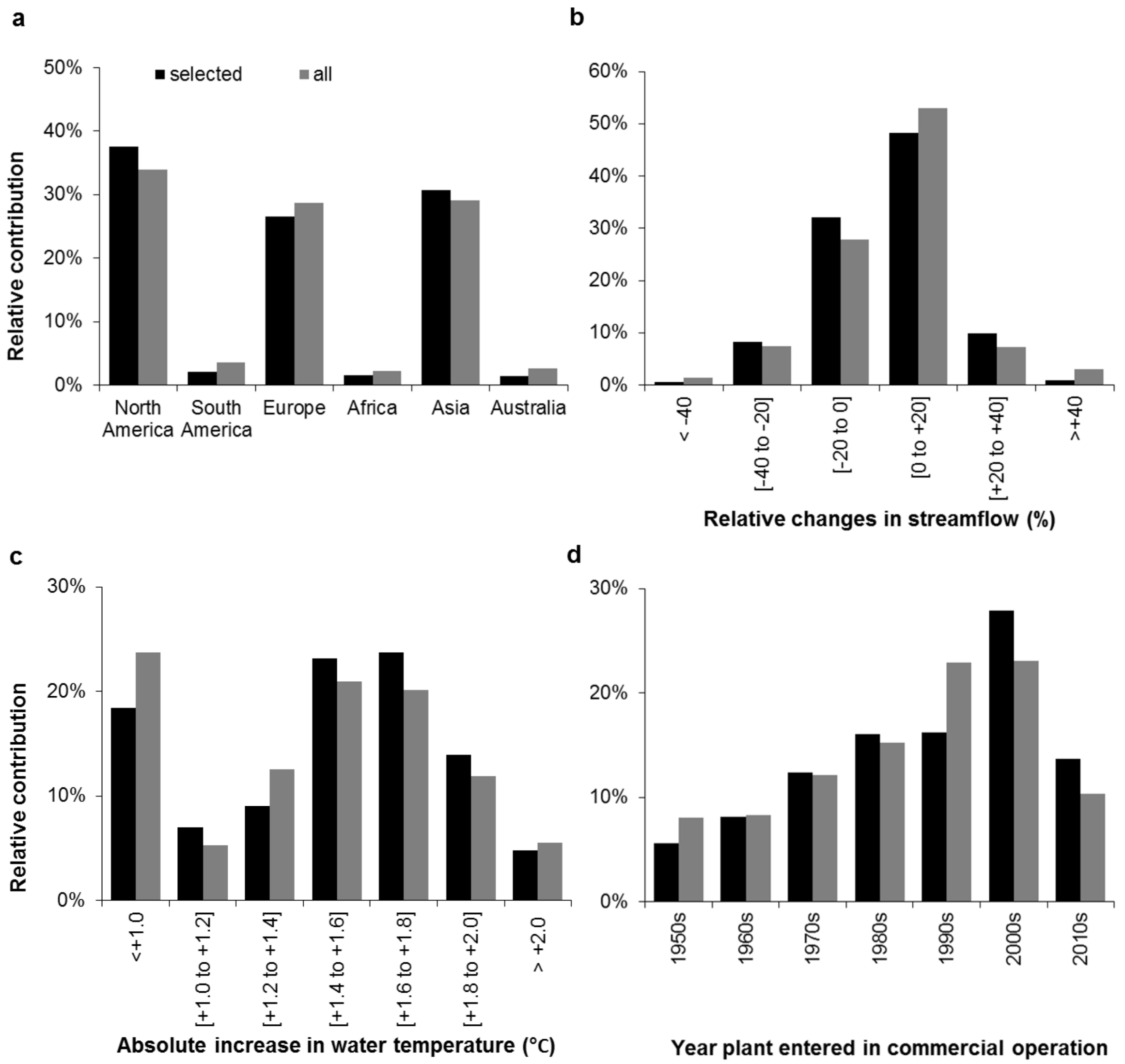

Figure S1: Comparison of 1,427 thermoelectric power plants of this study (black) and all 80,789 thermoelectric power plants from WEPPD for which latitude-longitude was assigned (grey). A comparison was made for geographic distribution per continent (**a**), relative change in streamflow (**b**) and absolute increase in water temperature (**c**) at power plant site under climate change (RCP8.5 for 2050s), and for the year that the plant entered in commercial operation (age distribution) (**d**).

For hydropower, we focused on a much larger number of plants (24,515) because fewer input parameters are required to describe the power plant characteristics in the hydropower model than for the thermoelectric power model. All hydropower plants together contribute 78% of the total installed hydropower usable capacity worldwide as reported by EIA[20]. A multiple regression model was used to derive hydraulic head. We merged information of the dam height reported by the Global Reservoir and Dam database (GRanD)[21] with the hydropower plants from the WEPPD based on exact corresponding latitude-longitude of hydropower plants between GRanD and WEPPD. We then fitted a multiple regression relation between dam height with installed capacity of the hydropower plant, elevation, differences in elevation with downstream located cell and simulated mean monthly lowest and highest streamflow for the grid cell at the hydropower plant site. To estimate elevation and elevation differences at each of the hydropower plant sites we use GTOPO30[22] at 30-arc seconds (1x1 km at the equator) spatial resolution. The multiple regression model was fitted for 390 hydropower plants and was used to assess the hydraulic head. The coefficient of determination of this model was moderate (R^2=0.51), but we considered this as acceptable given the global scale application, which restricts the availability of detailed data and use of more explanatory variables. In addition, sensitivity analyses show limited impacts of uncertainties in hydraulic head on simulated changes in hydropower usable capacity under climate change (see Section 3, Fig S9a).

For thermoelectric power, environmental water temperature limitations were derived at each power plant site with multiple regression models describing the relations of Tl_{max} and ΔTl_{max} with simulated mean naturalized water temperature (excluding impacts of heat effluents) and mean annual streamflow at the power plant site. These regression models were fitted for 529 thermoelectric power plants in the United States[23] for which Tl_{max} and ΔTl_{max} are reported and were applied to other thermoelectric power plants worldwide. The coefficient of determination of both regression models was moderate (R^2>0.3) but we considered this as acceptable for this global application. In addition, sensitivity analyses show overall limited impacts of uncertainties in estimated Tl_{max} and ΔTl_{max} on simulated changes in thermoelectric power usable capacity under climate change (see Section 3, Fig S9b-c). The multiple regression models describe that Tl_{max} increases when mean naturalized water temperatures and mean streamflow at the thermoelectric power plant site increases, taking variations in hydro-climatic conditions of thermoelectric plants over the world into account. ΔTl_{max} mainly increases when streamflow increases, describing an increase in dilution capacity for thermal effluents.

The selected power plants cover a broad range in installed capacities from 0.001 MW to 812 MW for hydropower (Fig S2a) and 1 MW to 6830 MW for thermoelectric power (Fig S2b). For thermoelectric power, plants with various sources of fuels are included: coal (45.7% for baseline settings), oil (3.4%), gas (32.1%), biomass (9.4%), nuclear (5.6%) and geothermal (3.8%) plants (Fig S3). For the baseline (present-day) power plant setting, 19.6% of the selected thermoelectric power plants use once-through (freshwater) cooling, 78.9% recirculation (wet tower) cooling and 1.5% combination cooling (once-through with supplementary tower) (Fig S4).

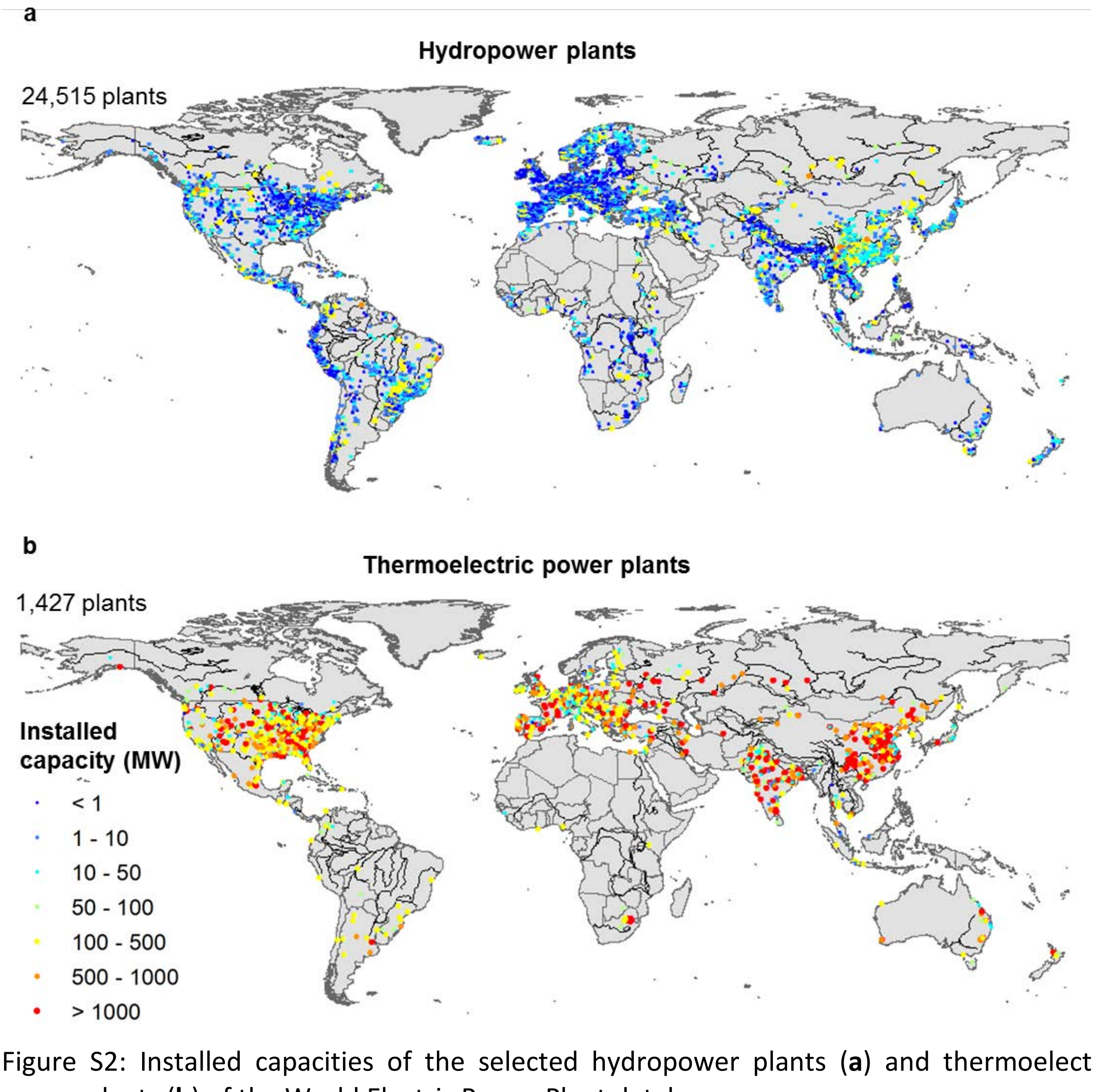

Figure S2: Installed capacities of the selected hydropower plants (**a**) and thermoelectric power plants (**b**) of the World Electric Power Plant database.

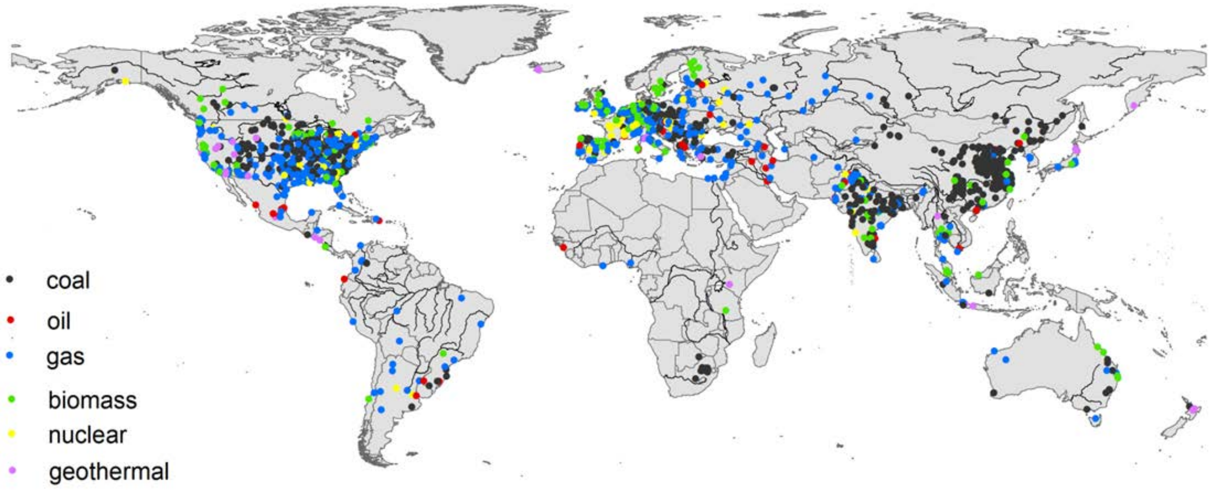

Figure S3: Source of fuel of selected thermoelectric power plants for baseline power plant settings

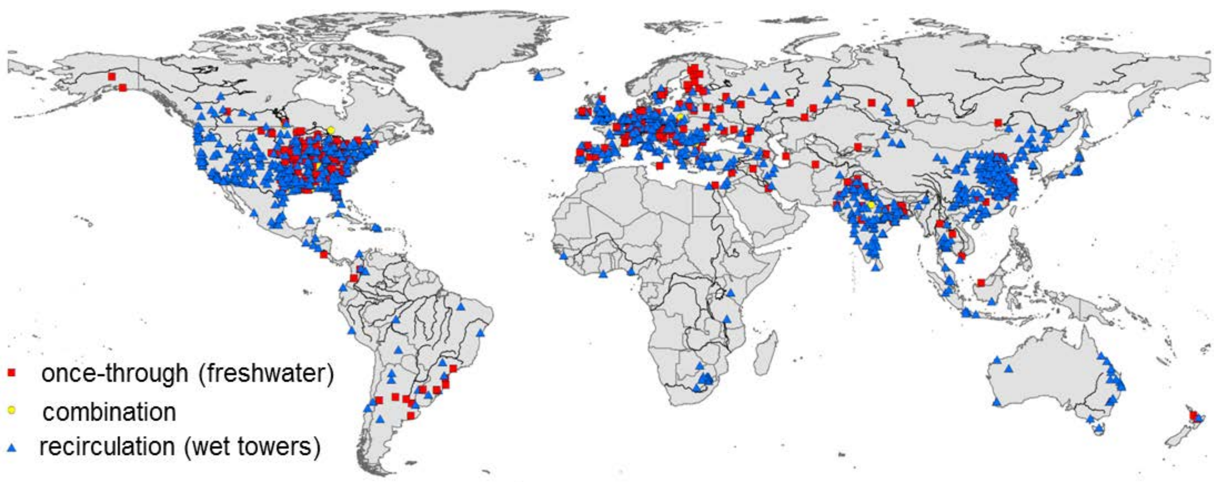

Figure S4: Cooling system type of selected thermoelectric power plants for baseline power plant settings

3) Performance and uncertainties of hydrological-electricity modelling framework

The performance of the coupled hydrological-electricity modelling framework was tested for the historical period 1981-2010 using the global WATCH Forcing Data Era Interim (WFDEI)[24] on 0.5°x0.5° resolution. We selected this period to evaluate the quality of our model simulations, because observed data of hydropower and thermoelectric power generation of EIA[20] were only available for the period after 1980. Daily streamflow and water temperature simulations were evaluated using observed streamflow records of 1,557 stations from the Global Runoff Data Centre (GRDC)[25] and daily water temperature of 438 stations from the UN Global Monitoring System (GEMS/Water)[26] combined with other sources (see van Vliet et al.[12]). For hydropower and thermoelectric power generation we used observed records of the Energy Information Administration (EIA)[20], which are only available on country level and on annual basis for 1981-2010. We therefore evaluated the simulations of hydropower and thermoelectric power generation by aggregating production potentials for all power plants within a country to annual basis. As only a selection of power plants is included in each country, simulated power generation had to be corrected by installed capacity to compare our simulations with the data of EIA. We therefore multiplied the sum of simulated power generation over all power plants in each country and year with the ratio of the total installed capacity reported by EIA and sum of installed capacity for all power plants in the country and for each year.

We calculated the root mean squared error (RMSE) and mean BIAS to assess the quality of the simulations of streamflow, water temperature, hydropower generation and thermoelectric power generation. For streamflow, hydropower generation and thermoelectric power generation, normalized values of RMSE and BIAS were calculated by dividing by the mean of observed values. Water temperature has a smaller variability worldwide and we therefore focused on absolute values of RMSE and BIAS.

The results of the model evaluation show an overall realistic representation of the observed conditions for 1981-2100. Normalized mean BIAS in streamflow was between -0.25 and +0.25 for 47% of the river stations worldwide (Fig S5). A slightly larger number of stations show a positive (54%) rather than negative (46%) normalized mean BIAS, which might be caused by neglect of water extractions and complicated wetland dynamics. Normalized 10-percentile (P10) BIAS was used to evaluate the performance of the model for low streamflow. Normalized P10 BIAS is for most stations slightly larger than the mean BIAS, with values between -0.25 and +0.25 for 33% and between -0.50 and +0.50 for 54% of the river stations worldwide. For water temperature, mean BIAS was between -1°C and +1°C for 49% and RMSE was smaller than 3°C for 53% of the river stations worldwide. The 90-percentile (P90) BIAS was calculated to assess the performance of the modelling framework for the high water temperature simulations. Although the P90 BIAS showed a slight overestimation of high water temperatures in the high latitude region and underestimation for some stations in the tropics, the performance distribution over all stations was comparable to the distribution in mean BIAS with values between -1°C and +1°C for 44% of the stations. Overall we found a lower performance for some river stations in the high latitude regions, however, the number of power plants situated in these regions is very small and this reduces the impacts of biases in water temperature on simulated thermoelectric power usable capacity.

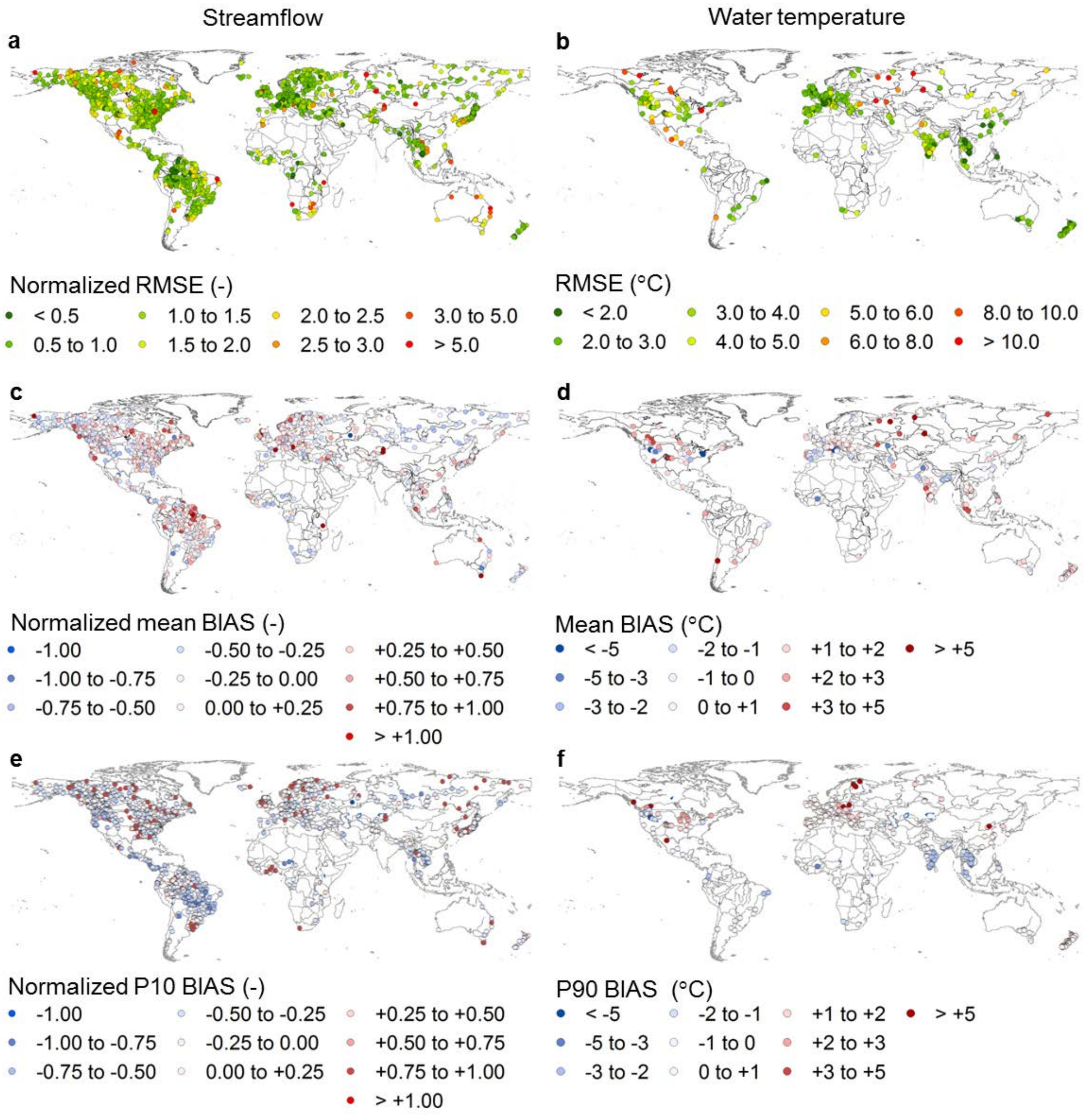

Figure S5: Performance of streamflow (**a,c,e**) and water temperature (**b,d,f**) modelling. Maps with calculated RMSE (**a,b**) and mean BIAS (**c,d**) are presented for the period 1981-2010 for monitoring stations worldwide. Normalized values of BIAS and RMSE are presented for streamflow. In addition, we present the normalized 10-percentile (P10) BIAS to assess the performance for low flow (**e**) and the 90-percentile (P90) BIAS for high water temperature (**f**) simulations.

Evaluation of the hydropower and thermoelectric power generation on county level shows small values of normalized BIAS (between -0.25 and +0.25) and normalized RMSE (smaller than 0.25) for most countries worldwide (Fig S6). Both the normalized BIAS and RMSE are slightly higher for countries in Africa. This is mainly because the interannual variability in simulated hydropower and thermoelectric power generation was slightly overestimated for some power plants and the number of plants over which the results are aggregated is low in most African countries (Fig S7). However, for most countries worldwide the hydrological-electricity modelling framework shows a realistic representation of the observed conditions. In addition, a comparison of the annual trends in simulated hydropower and thermoelectric power potential for 1981-2010 correspond closely with the observed trends reported by EIA[20] for most regions worldwide (Fig S8).

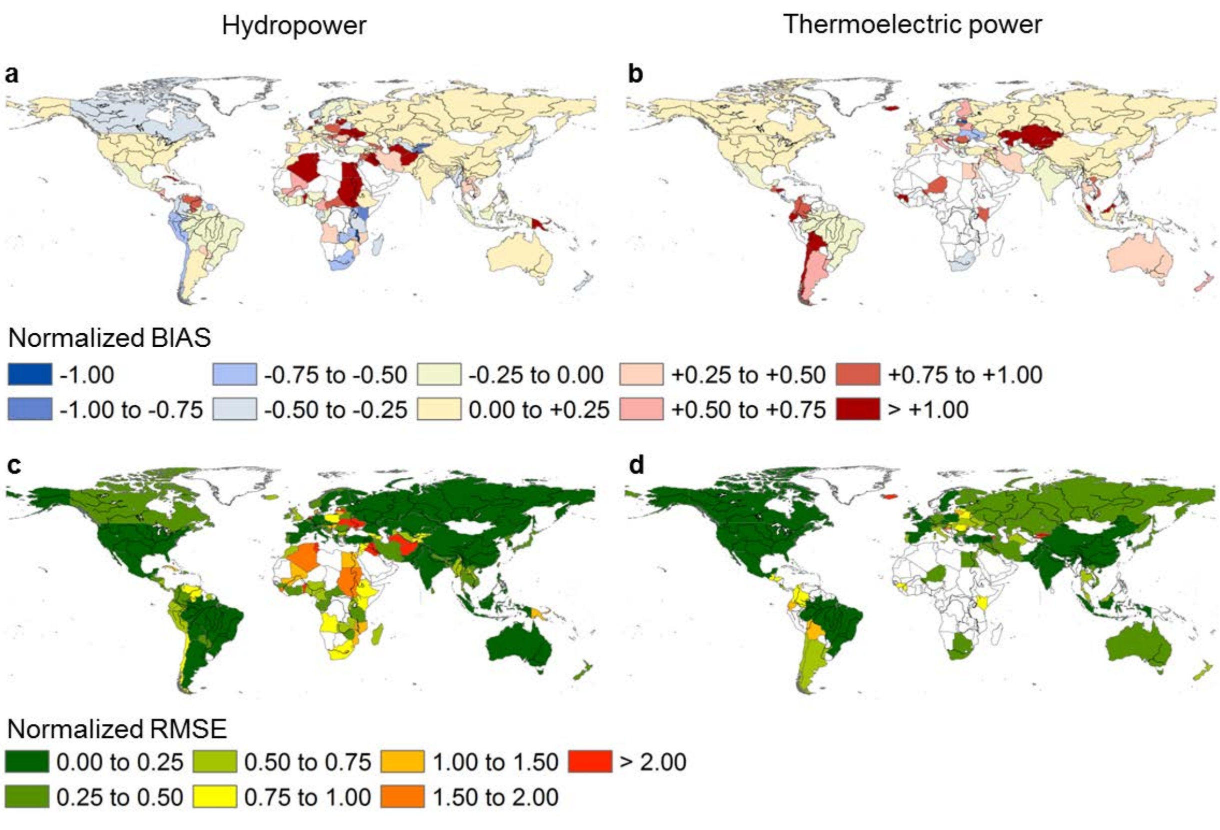

Figure S6: Performance of hydropower generation (**a,c**) and thermoelectric power generation (**b,d**) modelling. Maps with calculated normalized BIAS (**a,b**) and RMSE (**c,d**) are presented for the period 1981-2010 for countries where the selected power plants are situated.

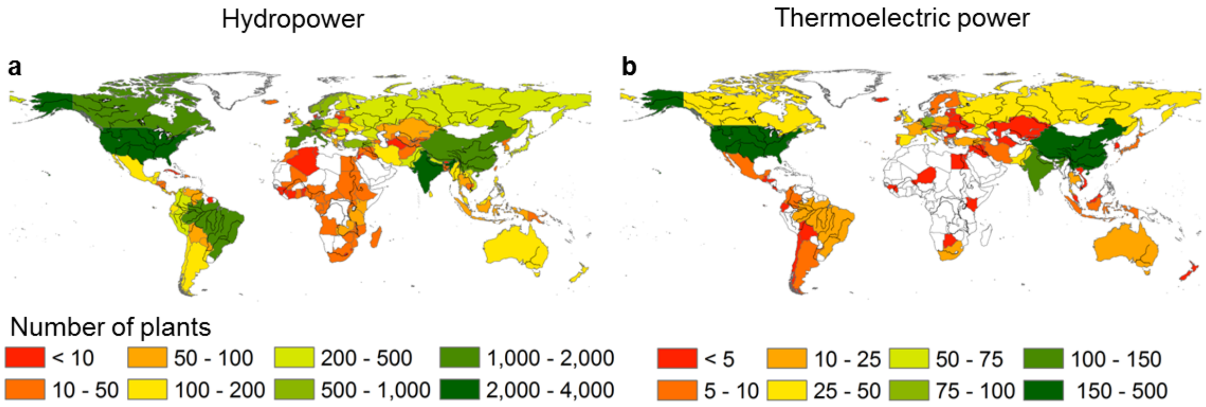

Figure S7: Number of hydropower power plants (**a**) and thermoelectric power plants (**b**) per country over which the results are aggregated for model evaluation purposes.

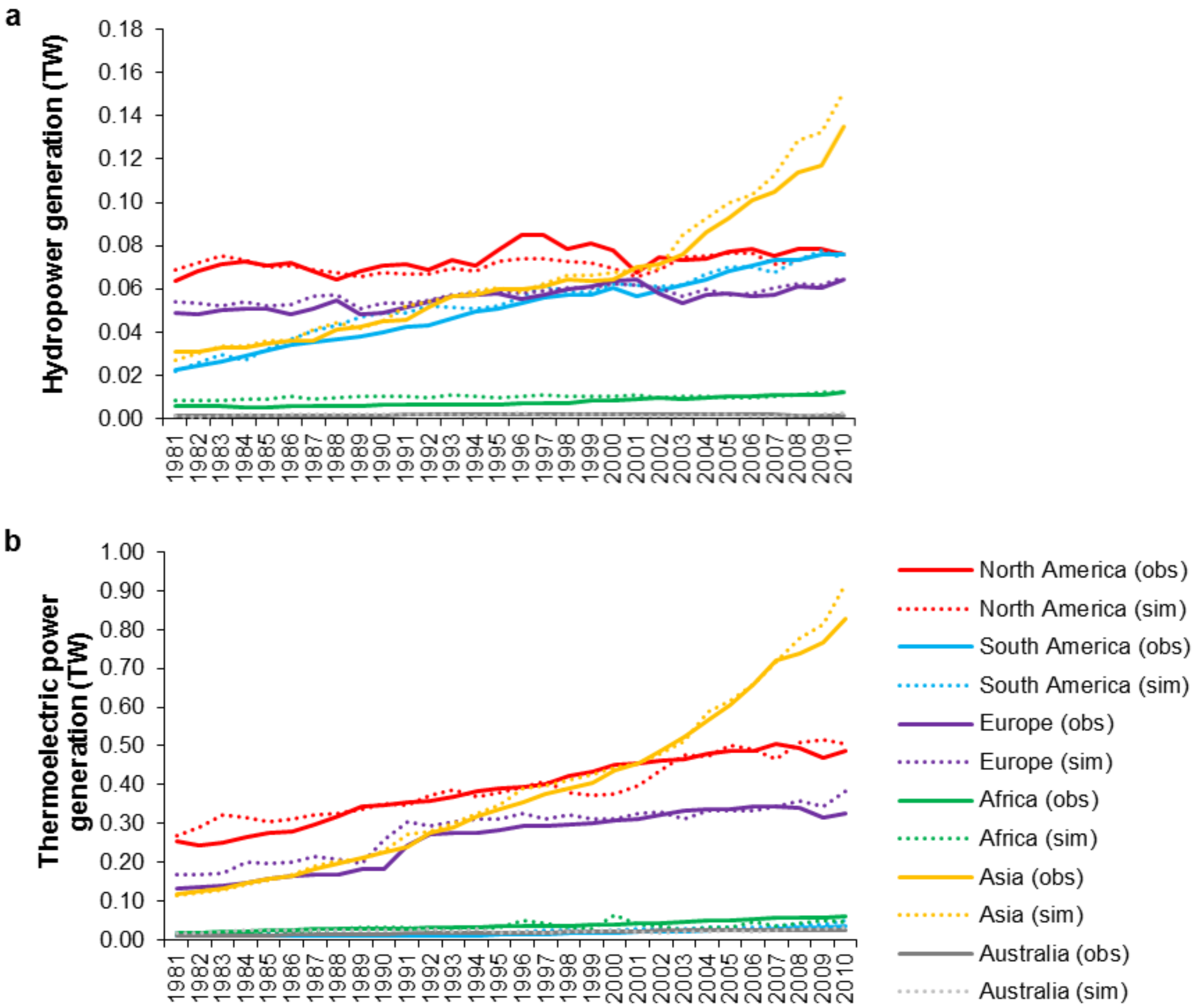

Figure S8: Comparison of annual trends in observed (obs; EIA) and simulated (sim) hydropower generation (**a**) and thermoelectric power generation (**b**) for 1981-2010 on continental level.

Sensitivity analyses were performed to study in more detail the impacts of uncertainties in the statistically-derived parameter estimates of hydraulic head (*H*) on simulated hydropower usable capacity and impacts of uncertainties in maximum permissible temperature of cooling water (Tl_{max}) and temperature increase of cooling water (ΔTl_{max}) on simulated thermoelectric power usable capacity. The impacts of parameter uncertainties on the main outcomes of this study were tested by performing additional simulations with the hydropower model and thermoelectric power model assuming both an increase and decrease in parameter estimates of *H*, Tl_{max} and ΔTl_{max} with 10% and 20%. Sensitivity runs were done for the historical period 1981-2000 based on the WFDEI meteorological dataset to assess the impacts of uncertainties in parameter estimates on absolute values of hydropower and thermoelectric power usable capacity. In addition, we performed sensitivity runs for all ten climate scenarios used in this study (see Section 4) to estimate how parameter uncertainties in *H*, Tl_{max} and ΔTl_{max} will impact the simulated changes in hydropower and thermoelectric power usable capacity under climate change.

We found that absolute values of simulated hydropower for 1981-2000 (based on WFDEI) are quite sensitive to parameter uncertainties of *H.* A decrease and increase in *H* of 20% changed the absolute values of hydropower usable capacity worldwide with -7.8% and +6.6%, respectively (see Table S1 for results of different continents). However, sensitivities of simulated changes in hydropower usable capacity under climate change to uncertainties in *H* estimates are very small. Sensitivity analyses for the climate scenarios show almost similar impacts of climate change on simulated hydropower usable capacity for different estimates of *H* (i.e. baseline value and under -20%, -10%, +10% and +20%) (see Fig S9a for RCP8.5 for the 2020s, 2050s and 2080s). The impacts on relative changes in hydropower usable capacity under climate change are limited, because uncertainties in *H* affect simulated hydropower usable capacity for both the future and control period.

Impacts of parameter uncertainties in Tl_{max} and ΔTl_{max} were studied in a similar way as for *H.* Parameter uncertainties in Tl_{max} have slightly stronger impacts on absolute values of simulated thermoelectric power usable capacity for 1981-2010 (based on WFDEI) than uncertainties in $\Delta Tl_{max.}$ A decrease and increase in Tl_{max} of 20% changed the absolute values of thermoelectric power usable capacity worldwide with -6.6% and +6.5% (Table S2), respectively, while this sensitivity was only -1.1% and +0.6% for ΔTl_{max} (Table S3). Slightly stronger sensitivities were also found for uncertainties in estimates of Tl_{max} compared to ΔTl_{max} for the simulated impacts of climate change on thermoelectric power usable capacity (see Fig S9b-c). However, uncertainties in H, Tl_{max} and ΔTl_{max} on hydropower and thermoelectric power usable capacities under climate change are overall small. This indicates limited effects of these parameter uncertainties on the main outcomes of this study.

Table S1: Impact of parameter uncertainties in hydraulic head (H) on simulated hydropower usable capacity for 1981-2000 assuming a deviation of -20%, -10%, +10% and +20% compared to the baseline value of H.

	H -20%	**H -10%**	**H +10%**	**H +20%**
North America	-5.8%	-2.7%	2.4%	4.7%
South America	-5.5%	-2.6%	2.4%	4.6%
Europe	-9.7%	-4.6%	4.3%	8.3%
Africa	-5.3%	-2.5%	2.2%	4.2%
Asia	-9.3%	-4.5%	4.1%	8.0%
Australia	-14.2%	-6.9%	6.5%	12.6%
World	-7.8%	-3.7%	3.4%	6.6%

Table S2: Impact of parameter uncertainties in maximum permissible temperature of cooling water (Tl_{max}) on simulated thermoelectric power usable capacity for 1981-2000 assuming a deviation of -20%, -10%, +10% and +20% compared to the baseline value of Tl_{max}.

	Tl_{max} -20%	**Tl_{max} -10%**	**Tl_{max} + 10%**	**Tl_{max} + 20%**
North America	-7.9%	-3.9%	3.6%	6.9%
South America	-4.0%	-2.0%	2.6%	6.2%
Europe	-8.6%	-4.5%	4.8%	9.1%
Africa	-7.4%	-2.9%	2.1%	3.6%
Asia	-4.1%	-2.0%	2.2%	4.8%
Australia	-4.5%	-2.0%	1.6%	3.0%
World	-6.6%	-3.3%	3.3%	6.5%

Table S3: Impact of parameter uncertainties in maximum permissible temperature increase of cooling water (ΔTl_{max}) on simulated thermoelectric power usable capacity for 1981-2000 assuming a deviation of -20%, -10%, +10% and +20% compared to the baseline value of ΔTl_{max}.

	ΔTl_{max} -20%	**ΔTl_{max} -10%**	**ΔTl_{max} +10%**	**ΔTl_{max} +20%**
North America	-1.1%	-0.5%	0.4%	0.6%
South America	-2.6%	-1.2%	1.0%	1.6%
Europe	-0.4%	-0.2%	0.1%	0.1%
Africa	-3.4%	-1.5%	1.2%	1.9%
Asia	-1.5%	-0.7%	0.5%	0.9%
Australia	-1.6%	-0.6%	0.3%	0.5%
World	-1.1%	-0.5%	0.4%	0.6%

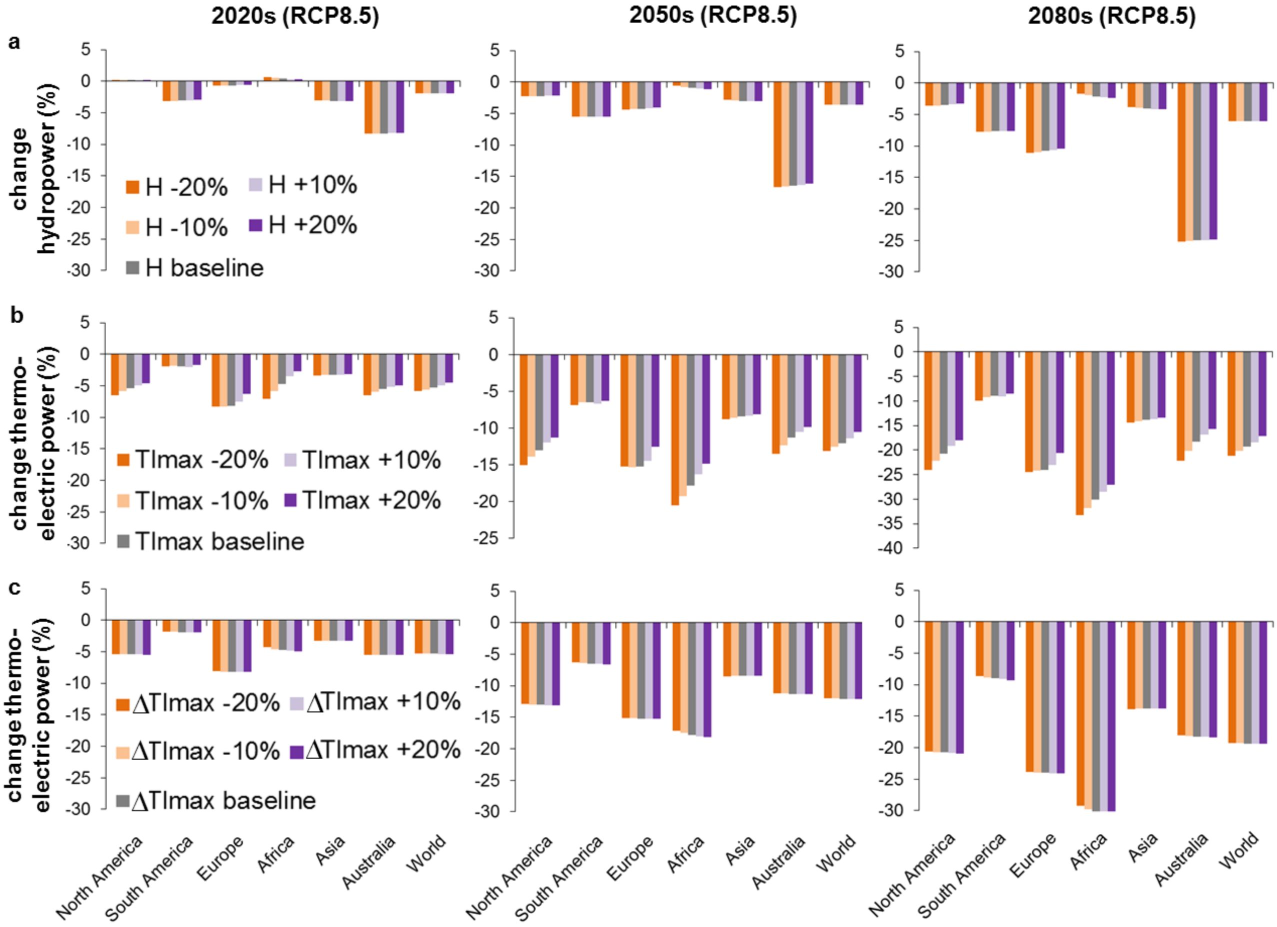

Figure S9: Impacts of parameter uncertainties in hydraulic head (*H*) on simulated changes in hydropower usable capacity under climate change (**a**); and impacts of parameter uncertainties in maximum permissible temperature of cooling water (Tl_{max}) (**b**) and maximum permissible temperature increase of cooling water (ΔTl_{max}) (**c**) on simulated changes in thermoelectric power usable capacity for RCP8.5 for the 2020s, 2050s and 2080s.

4) Climate scenarios

The coupled hydrological-electricity modelling framework was forced with bias-corrected climate forcing[27] of five general circulation models (GCMs): MIROC-ESM-CHEM, IPSL-CM5A-LR, HadGEM2-ES, NorESM1-M and GFDL-ESM2M. We used the GCM experiments for the representative concentration pathways (RCPs) 2.6[28] and 8.5[29] for 1971-2099, capturing the largest range of uncertainties in the state-of-the-art future greenhouse gas concentration scenarios. RCP2.6 has a peak in radiative forcing at ~3 W/m^2 (~490 ppm CO_2 eq) before 2100 and then declines to 2.6 W/m^2 by 2100 [28,30]. RCP8.5 describes a rising radiative forcing pathway leading to 8.5 W/m^2 (~1370 ppm CO_2 eq) by 2100 [29,30]. Global simulations of streamflow and water temperature were produced on daily time step and on 0.5°x0.5° spatial resolution for all ten GCM experiments.

5) Adaptation options to reduce the vulnerability to water constraints under climate change

To assess effective strategies for reducing the vulnerability of world's current hydropower and thermoelectric power generation system to climate change and increasing water constraints, we tested a set of six adaptation options which are discussed below.

1. Increases in total efficiencies of hydropower plants

For all hydropower plants in this study we assumed that the total efficiency, which includes both the efficiency of the turbine and the efficiency of the generator, will be increased by 10%. This 10% value was assumed as an upper range in total hydropower plant efficiency increase. The present-day total efficiencies of hydropower plants vary mainly depending on type, age of turbines and generators and installed capacity[31]. For some hydropower plants in our dataset increases in total efficiency of 10% are more likely than for others. However, due to uncertainties in various drivers affecting technological developments and changes in plant efficiencies we assumed a constant 10% increase for all hydropower plants.

2. Increases in total efficiencies of thermoelectric power plants

For this adaptation option, we assumed an increase in total efficiency of 20% for all thermoelectric power plants. This 20% value was considered as an upper range of thermoelectric power efficiency increase. Present-day efficiencies of thermoelectric power plants depend mainly on technology (source of fuel) and age of the power plant[32]. Due to uncertainties in various drivers affecting future technological changes, we assumed a constant increase of 20% which was applied to the present-day efficiency values of all thermoelectric power plants in our dataset. For more than 95% of the thermoelectric power plants in our dataset the efficiency value under this adaptation option is still lower than the highest plant efficiency value under baseline settings. Thermoelectric power plant vulnerabilities to water constraints under climate change were also tested under a smaller increase in total efficiency of 10% for all thermoelectric power plants (see Fig S10). The reduction in vulnerability of thermoelectric power plants to water constraints is slightly lower for a 10% efficiency increase than for a 20% efficiency increase. However, increases in power plant efficiencies of both 10% and 20% are for most regions still insufficient to mitigate overall reductions in cooling water use potential under changing climate.

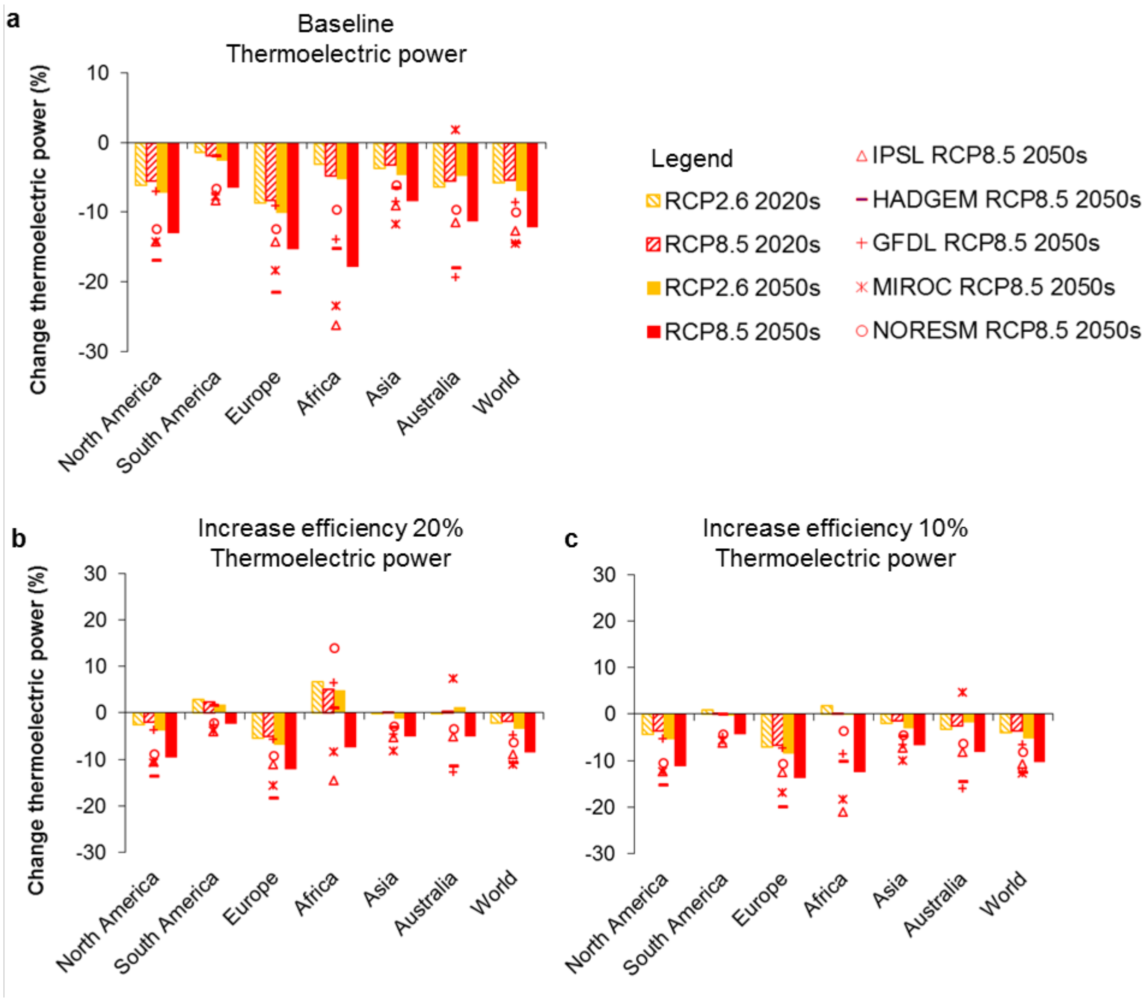

Figure S10: Impacts of increases in plant efficiencies on the vulnerability of thermoelectric power usable capacity to water constraints under climate change (**a,b,c**). Results for the baseline power plant settings (**a**), under efficiency increase of 20% (**b**) and under a lower assumed value of increase in plant efficiency (10%) (**c**). Results for the baseline power plant settings and under efficiency increase of 20% are also presented in Figure 4b (main text) and are included here for comparison.

3. Replacement of fuel sources of thermoelectric power plants

The assumption was made that all coal- and oil-fired plants are replaced by gas-fired power plants (see Fig S3 for baseline settings). It should be mentioned that a replacement of nuclear and biomass-fuelled power plants, which have overall lower efficiencies and therefore higher cooling water demands than coal- and oil-fired plants, might be more effective in reducing thermoelectric water demands[33,34]. However, global assessments of future energy mixes mainly show increases in nuclear and biomass and overall decreases in the contributions of coal and oil for power generation[33] because enforcement of climate change mitigation policies warrants a reduction in coal- and oil-fired plants. We therefore decided to test as an adaptation option a replacement of coal- and oil-fired plants by gas-fired plants.

4. Switch to recirculation (wet tower) cooling system of thermoelectric power plants

For this adaptation option, we assumed that thermoelectric power plants with once-through cooling systems are replaced by recirculation (wet tower) cooling systems (see Fig S4 for baseline settings). A switch from once-through to recirculation cooling decreases surface water withdrawal and therefore reduces power plant vulnerabilities to water constraints. It should however be mentioned that a switch to recirculation cooling will slightly increase water consumption (due to evaporative losses in cooling towers) compared to once-through systems[16].

5. Switch to sea water cooling for thermoelectric power plants along the coast

For this adaptation option we calculated how a switch to sea water cooling of power plants nearby the coast will reduce the impacts of freshwater constraints on thermoelectric power usable capacity. We assumed that all thermoelectric power plants within a range of 100 km from the coastal line will switch to sea water cooling. This range of 100 km is considered as an upper bound and was assessed based on literature[35] and information for water transport distances of existing thermoelectric power plants, such as those in Arizona (United States) for which current distances of 70 km are reported[36]. Distances may vary locally, and probably depend on various factors, e.g. future costs and availability of energy for conveying sea water, local cross-sectoral competition of freshwater resources with other sectors (e.g. agriculture, domestic uses) and also geographic (coastal) conditions and developments. In total 313 thermoelectric power plants in our dataset (22%) are located within this 100 km range and all these plants were assumed to switch to sea water cooling (see Fig S11).

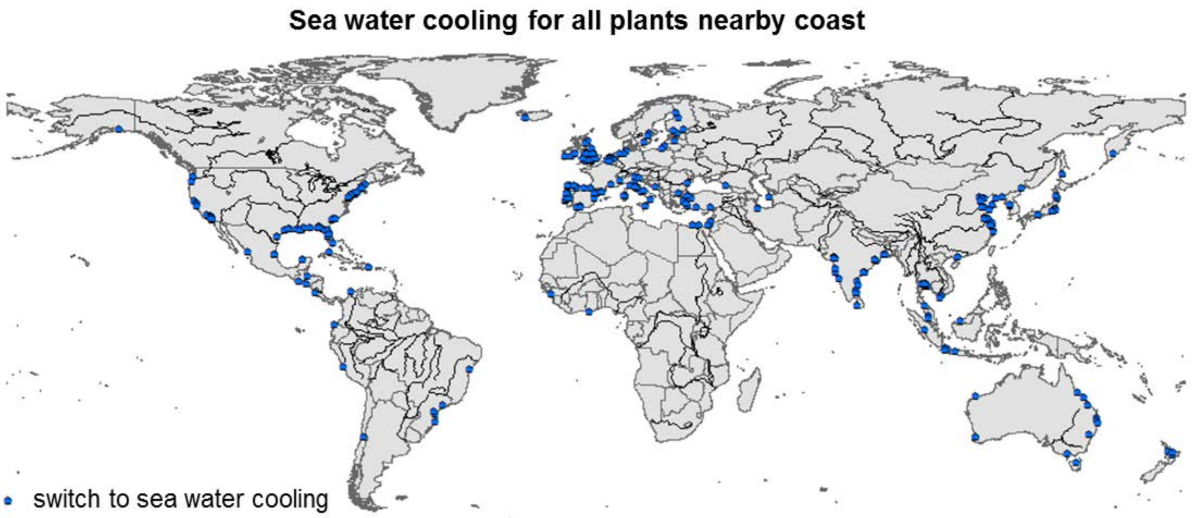

Figure S11: Location of thermoelectric power plants within 100 km distance from the coast for which a switch to sea water cooling was tested as adaptation option.

6. Decoupling from freshwater resources for most vulnerable thermoelectric power plants

We tested a decoupling of thermoelectric power plants from freshwater resources for 10% of the thermoelectric power plants (n=143), which were most severely impacted by water constraints under climate change. We thus assumed that power plants which are most severely impacted by climate change and changes in water resources are more likely to adapt, because large investments for adaptation might be more profitable than for thermoelectric power plants with moderate impacts. This decoupling from freshwater resources for the most vulnerable thermoelectric power plants could potentially be obtained by using sea water cooling and dry (air) cooling systems as alternative. We assumed that vulnerable thermoelectric power plants within a 100 km range from the coastal line are likely to switch to sea water cooling (n=26; 1.8%) as alternative. The remaining, inland located plants were assumed to switch to dry (air) cooling (n=117; 8.2%) (see Fig S12). For plants switching to dry cooling, we included an efficiency loss of 6% in our model simulations. This is the median value based on the efficiency loss range of 2-10% reported by Stillwell and Webber[37].

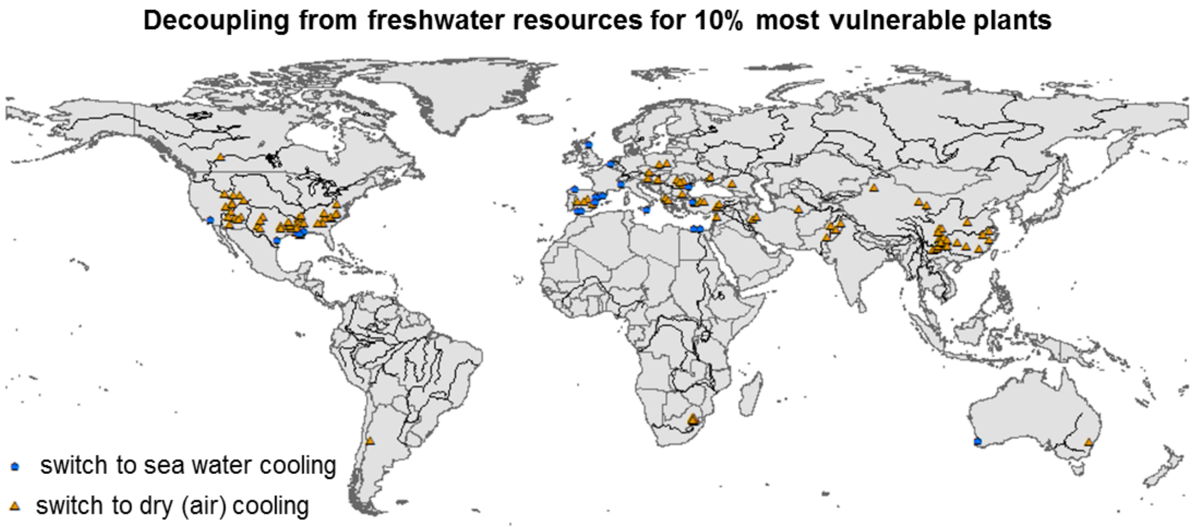

Figure S12: Location of the 10% thermoelectric power plants that are most vulnerable to water constraints under climate change for which decoupling from freshwater resources was tested as adaptation option. A switch to sea water cooling was assumed for thermoelectric power plants within 100 km distance from the coast and a switch to dry (air) cooling for inland located plants.

All adaptation options were assumed to occur as sudden shifts during the start of the 2020s period. Although these shifts are not meant to be realistic representations of the diffusion speed of technological changes, it allow us to directly assess the impacts of these adaptation options on the vulnerability to water constraints for future time slices compared to the control period.

In addition to the results presented in the main text an overview of the impacts of climate change on mean annual usable power plant capacity for hydropower (Table S4) and thermoelectric power (Table S5) is presented for the baseline power plant setting and for various adaptation options. We show the impacts on GCM ensemble mean and GCM range (minimum-maximum) based on all five GCMs for RCP2.6 and RCP8.5. Differences between impacts of various adaptation options on usable power plant capacities are discussed in the main text. Below we focus also on the range in impacts for the five different GCMs. For the baseline power plant settings, we found for most regions overall stronger declines in hydropower and thermoelectric power usable capacity for the GCM experiments of MIROC, IPSL and HADGEM than for GFDL and NORESM. This difference between the GCMs is also in line with the projected impacts on global mean temperature by this set of GCMs[38]. As expected, impacts of water constraints on usable power plant capacities are larger for RCP8.5 than for RCP2.6, in particular from the mid-century (2050s) when the greenhouse gas concentrations for both RCPs further deviate[39]. For all six adaptation options we found a reduced vulnerability of the electricity sector to water constraints under climate change. The range between the different GCM experiments for these adaptation options was comparable to the range found for the baseline settings. For all five GCM experiments, consistently higher values of usable power plant capacities were found for the adaptation options compared to the baseline settings. This indicates for each of the adaptation options robustness in the simulated reductions of vulnerability to water constraints under climate change.

Table S4: Climate change impacts on mean annual usable capacity of hydropower for the baseline power plant settings and under an increase in efficiency of 10% (incr. eff. 10%) as adaptation option. Relative (%) changes in GCM ensemble mean and GCM range (minimum-maximum) based on all five GCMs are presented.

	RCP 2.6 2020s **GCM mean** [range]		**RCP 2.6 2050s** **GCM mean** [range]		**RCP 8.5 2020s** **GCM mean** [range]		**RCP 8.5 2050s** **GCM mean** [range]	
North America								
baseline	**-0.1**	[-1.3, 0.6]	**0.4**	[-2.0 , 1.3]	**0.2**	[-2.0, 1.5]	**-2.2**	[-5.5, -0.3]
incr. eff. 10%	**2.4**	[1.2, 3.0]	**2.8**	[0.5, 3.8]	**2.7**	[0.5, 3.9]	**0.2**	[-3.0, 2.1]
South America								
baseline	**-2.8**	[-7.9, 0.5]	**-3.7**	[-8.7, 0.9]	**-3.1**	[-6.5, -0.1]	**-5.5**	[-12.4, 0.7]
incr. eff. 10%	**-0.5**	[-5.6, 2.8]	**-1.4**	[-6.4, 3.2]	**-0.7**	[-4.1, 2.2]	**-3.2**	[-10.2, 2.9]
Europe								
baseline	**-1.5**	[-4.7, 0.7]	**-0.1**	[-3.4, 2.0]	**-0.7**	[-2.7, 2.7]	**-4.2**	[-10.8, -0.5]
incr. eff. 10%	**2.8**	[-0.5, 5.0]	**4.2**	[0.8, 6.4]	**3.6**	[1.5, 7.1]	**-0.1**	[-6.8, 3.8]
Africa								
baseline	**0.1**	[-1.6, 0.8]	**-0.9**	[-2.7, 0.3]	**0.4**	[-0.7, 1.0]	**-0.9**	[-3.2, 3.0]
incr. eff. 10%	**2.2**	[0.7, 3.0]	**1.2**	[-0.5, 2.3]	**2.6**	[1.5, 3.2]	**1.2**	[-1.1, 5.2]
Asia								
baseline	**-2.2**	[-3.8, -1.2]	**-0.9**	[-3.4, 2.6]	**-3.1**	[-4.3, -1.7]	**-3.0**	[-5.8, -0.4]
incr. eff. 10%	**1.8**	[0.2, 2.9]	**3.1**	[0.6, 6.7]	**0.9**	[-0.3, 2.3]	**1.0**	[-1.9, 3.6]
Australia								
baseline	**-10.4**	[-16.4, 3.1]	**-6.4**	[-16.1, 10.1]	**-8.3**	[-15.3, 4.8]	**-16.4**	[-27.1, 11.6]
incr. eff. 10%	**-4.5**	[-11.1, 10.0]	**-0.4**	[-10.6, 17.4]	**-2.3**	[-9.9, 11.9]	**-10.9**	[-22.4, 19.1]
World								
baseline	**-1.7**	[-2.7, -0.6]	**-1.2**	[-2.5, 1.0]	**-1.9**	[-2.6, -0.8]	**-3.6**	[-5.2, -2.4]
incr. eff. 10%	**1.6**	[0.6, 2.8]	**2.2**	[0.8, 4.5]	**1.5**	[0.7, 2.5]	**-0.3**	[-2.0, 1.0]

Table S5: Climate change impacts on mean annual usable capacity of thermoelectric power for the baseline power plant setting and for various adaptation options for different regions. We tested the impacts of an increase in efficiency of 20% (incr. eff. 20%), change in source of fuel (change fuel), switch from once-through to recirculation (wet tower) cooling (switch tower cool), a switch from freshwater to sea water cooling for plants near the coast (switch sea cool), a decoupling from freshwater by switching to sea water or dry (air) cooling for 10% of thermoelectric power plants that are most vulnerable to water constraints under climate change (decoup. 10% vuln.). Relative (%) changes in GCM ensemble mean and GCM range (minimum-maximum) based on all five GCMs are presented.

	RCP 2.6 2020s		**RCP 2.6 2050s**		**RCP 8.5 2020s**		**RCP 8.5 2050s**	
	GCM mean	[range]	**GCM mean**	[range]	**GCM mean**	[range]	**GCM mean**	[range]
North America								
baseline	**-6.1**	[-8.3, -4.4]	**-7.2**	[-9.3, -3.8]	**-5.4**	[-6.5, -2.9]	**-13.0**	[-17.0, -7.0]
incr. eff. 20%	**-2.5**	[-4.8, -1.0]	**-3.7**	[-5.9, -0.3]	**-1.9**	[-3.0, 0.5]	**-9.5**	[-13.7, -3.7]
change fuel	**1.5**	[-1.0, 2.8]	**0.2**	[-2.3, 3.5]	**2.0**	[0.9, 4.2]	**-5.7**	[-10.0, -0.1]
switch tower cool	**4.9**	[2.3, 6.3]	**3.7**	[1.1, 7.3]	**5.4**	[4.2, 7.9]	**-2.6**	[-7.2, 3.3]
switch sea cool	**-1.9**	[-4.0, -0.2]	**-3.0**	[-5.0, 0.4]	**-1.3**	[-2.4, 1.2]	**-8.5**	[-12.2, -2.7]
decoup. 10% vuln.	**10.3**	[8.3, 11.3]	**9.4**	[7.2, 11.9]	**10.7**	[9.7, 12.3]	**4.6**	[0.8, 9.2]
South America								
baseline	**-1.3**	[-3.4, 0.7]	**-2.6**	[-4.9, -0.9]	**-1.9**	[-4.2, 0.6]	**-6.5**	[-8.4, -1.9]
incr. eff. 20%	**3.1**	[1.4, 5.4]	**1.8**	[-0.8, 3.3]	**2.4**	[0.0, 4.6]	**-2.3**	[-4.1, 1.6]
change fuel	**7.9**	[7.0, 10.1]	**6.7**	[4.7, 8.2]	**7.0**	[5.4, 8.7]	**3.1**	[1.5, 5.1]
switch tower cool	**20.3**	[18.4, 22.7]	**19.3**	[17.8, 21.5]	**19.5**	[18.2, 22.5]	**16.9**	[14.4, 19.3]
switch sea cool	**4.5**	[3.2, 6.0]	**3.3**	[1.7, 6.0]	**3.4**	[1.9, 4.5]	**0.2**	[-2.0, 3.2]
decoup. 10% vuln.	**-0.4**	[-2.4, 1.4]	**-1.5**	[-3.6, -0.1]	**-1.0**	[-2.9, 1.0]	**-4.9**	[-6.6, -0.9]
Europe								
baseline	**-8.6**	[-14.0, -4.3]	**-10.0**	[-15.0, -2.8]	**-8.2**	[-12.7, -4.2]	**-15.2**	[-21.5, -9.1]
incr. eff. 20%	**-5.4**	[-10.9, -0.8]	**-6.9**	[-12.1, 0.5]	**-5.0**	[-9.7, -0.9]	**-12.2**	[-18.5, -5.8]
change fuel	**-2.9**	[-8.4, 1.8]	**-4.4**	[-10.0, 3.1]	**-2.6**	[-7.3, 1.6]	**-9.8**	[-16.2, -3.2]
switch tower cool	**3.0**	[-3.0, 8.0]	**1.5**	[-3.9, 9.3]	**3.3**	[-1.7, 7.8]	**-4.0**	[-10.7, 2.7]
switch sea cool	**-0.8**	[-5.8, 3.0]	**-1.9**	[-6.5, 4.2]	**-0.4**	[-4.7, 2.9]	**-6.2**	[-11.8, -1.1]
decoup. 10% vuln.	**8.9**	[3.7, 13.1]	**7.7**	[3.0, 14.1]	**9.2**	[4.7, 12.9]	**3.6**	[-2.2, 9.2]
Africa								
baseline	**-3.1**	[-5.4, -1.6]	**-5.2**	[-10.8, 3.7]	**-4.8**	[-13.5, 7.4]	**-17.8**	[-26.3, -9.8]
incr. eff. 20%	**6.7**	[-19.9, 26.9]	**4.8**	[-12.6, 34.8]	**5.1**	[-8.8, 39.4]	**-7.3**	[-14.6, 13.8]
change fuel	**24.2**	[19.8, 28.0]	**22.9**	[16.2, 30.8]	**23.1**	[16.3, 34.0]	**13.1**	[5.6, 23.5]
switch tower cool	**-3.0**	[-5.3, -1.6]	**-5.2**	[-10.8, 3.7]	**-4.7**	[-13.5, 7.4]	**-17.8**	[-26.3, -9.7]
switch sea cool	**0.5**	[-1.9, 1.8]	**-1.7**	[-7.3, 7.3]	**-1.2**	[-9.9, 11.0]	**-14.2**	[-22.6, -6.2]
decoup. 10% vuln.	**19.1**	[16.1, 21.5]	**18.7**	[14.2, 22.4]	**18.2**	[15.0, 22.6]	**15.8**	[10.9, 20.2]

	RCP 2.6 2020s **GCM mean** [range]		RCP 2.6 2050s **GCM mean** [range]		RCP 8.5 2020s **GCM mean** [range]		RCP 8.5 2050s **GCM mean** [range]	
Asia								
baseline	**-3.6**	[-5.0, -1.9]	**-4.7**	[-7.4, -1.9]	**-3.2**	[-4.7, -1.2]	**-8.4**	[-11.7, -6.2]
incr. eff. 20%	**0.0**	[-1.5, 1.6]	**-1.2**	[-4.0, 1.6]	**0.4**	[-1.2, 2.3]	**-4.9**	[-8.3, -3.0]
change fuel	**5.0**	[3.4, 6.5]	**3.8**	[0.8, 6.2]	**5.4**	[3.7, 7.0]	**0.0**	[-3.4, 1.6]
switch tower cool	**3.3**	[1.8, 5.2]	**2.1**	[-0.8, 5.2]	**3.6**	[2.1, 5.8]	**-1.6**	[-5.1, 0.4]
switch sea cool	**2.7**	[1.0, 4.7]	**1.7**	[-1.2, 4.8]	**3.0**	[1.3, 5.5]	**-1.6**	[-4.9, 0.4]
decoup. 10% vuln.	**1.9**	[0.6, 3.8]	**1.3**	[-1.2, 4.2]	**2.4**	[0.9, 4.4]	**-1.6**	[-4.7, 0.3]
Australia								
baseline	**-6.3**	[-9.8, -0.1]	**-4.8**	[-10.4, 4.8]	**-5.5**	[-9.2, -0.3]	**-11.3**	[-19.3, 1.7]
incr. eff. 20%	**-0.2**	[-3.4, 6.0]	**1.1**	[-3.9, 10]	**0.5**	[-3.2, 5.7]	**-5.1**	[-12.8, 7.3]
change fuel	**10.7**	[8.0, 16.2]	**11.7**	[8.1, 18.7]	**11.2**	[8.0, 15.9]	**6.5**	[-0.2, 16.7]
switch tower cool	**-6.3**	[-9.8, -0.1]	**-4.8**	[-10.4, 4.8]	**-5.5**	[-9.2, -0.3]	**-11.3**	[-19.3, 1.7]
switch sea cool	**3.4**	[-0.5, 8.7]	**5.0**	[0.3, 13.4]	**4.3**	[0.4, 8.6]	**0.2**	[-6.9, 12.2]
decoup. 10% vuln.	**19.2**	[16.4, 22.1]	**20.2**	[18.1, 24.8]	**19.4**	[16.8, 22.3]	**17.2**	[12.5, 24.8]
World								
baseline	**-5.8**	[-7.4, -4.5]	**-7.0**	[-9.9, -4.3]	**-5.3**	[-6.6, -3.3]	**-12.1**	[-14.5, -8.6]
incr. eff. 20%	**-2.1**	[-3.8, -0.7]	**-3.3**	[-6.4, -0.6]	**-1.7**	[-3.1, 0.3]	**-8.5**	[-11.1, -4.9]
change fuel	**2.5**	[0.5, 3.8]	**1.2**	[-2.0, 4.1]	**2.8**	[1.2, 4.7]	**-4.0**	[-6.8, -0.3]
switch tower cool	**3.7**	[1.8, 5.1]	**2.4**	[-0.7, 5.3]	**4.0**	[2.6, 6.2]	**-2.9**	[-5.7, 0.8]
switch sea cool	**1.0**	[-0.5, 2.2]	**-0.1**	[-2.9, 2.3]	**1.3**	[-0.1, 3.1]	**-4.6**	[-7.0, -1.4]
decoup. 10% vuln.	**8.2**	[6.8, 9.4]	**7.4**	[4.8, 9.2]	**8.6**	[7.1, 10.0]	**3.7**	[1.3, 6.4]

References

1 Liang, X., Lettenmaier, D. P., Wood, E. F. & Burges, S. J. A Simple Hydrologically Based Model of Land-Surface Water and Energy Fluxes for General-Circulation Models. *Journal of Geophysical Research-Atmospheres* **99**, 14415-14428 (1994).

2 Nijssen, B., O'Donnell, G. M., Lettenmaier, D. P., Lohmann, D. & Wood, E. F. Predicting the discharge of global rivers. *Journal of Climate* **14**, 3307-3323 (2001).

3 Döll, P. & Lehner, B. Validation of a new global 30-min drainage direction map. *Journal of Hydrology* **258**, 214-231 (2002).

4 Haddeland, I., Skaugen, T. & Lettenmaier, D. P. Anthropogenic impacts on continental surface water fluxes. *Geophysical Research Letters* **33**, L08406, doi:10.1029/2006GL026047 (2006).

5 Lohmann, D., Raschke, E., Nijssen, B. & Lettenmaier, D. P. Regional scale hydrology: I. Formulation of the VIC-2L model coupled to a routing model. *Hydrological Sciences Journal-Journal Des Sciences Hydrologiques* **43**, 131-141 (1998).

6 Vrugt, J. A., Gupta, H. V., Bouten, W. & Sorooshian, S. C. A Shuffled Complex Evolution Metropolis algorithm for optimization and uncertainty assessment of hydrologic model parameters. *Water Resources Research* **39**, doi:10.1029/2002wr001642 (2003).

7 Haddeland, I., Skaugen, T. & Lettenmaier, D. P. Hydrologic effects of land and water management in North America and Asia: 1700-1992. *Hydrology and Earth System Sciences* **11**, 1035-1045 (2007).

8 Haddeland, I. *et al.* Global water resources affected by human interventions and climate change. *Proceedings of the National Academy of Sciences* **111**, 3251-3256, doi:10.1073/pnas.1222475110 (2014).

9 Adam, J. C., Haddeland, I., Su, F. & Lettenmaier, D. P. Simulation of reservoir influences on annual and seasonal streamflow changes for the Lena, Yenisei, and Ob' rivers. *Journal of Geophysical Research-Atmospheres* **112** (2007).

10 Yearsley, J. R. A semi-Lagrangian water temperature model for advection-dominated river systems. *Water Resources Research* **45** doi:10.1029/2008WR007629 (2009).

11 Yearsley, J. R. A grid-based approach for simulating stream temperature. *Water Resources Research* **48**, doi:10.1029/2011WR011515 (2012).

12 van Vliet, M. T. H. *et al.* Coupled Daily Streamflow and Water Temperature Modelling in Large River Basins. *Hydrol. Earth Syst. Sci.* **16**, 4303–4321, doi:10.5194/hess-16-4303-2012 (2012).

13 van Vliet, M. T. H. *et al.* Vulnerability of US and European electricity supply to climate change. *Nature Climate Change* **2**, 676-681, doi:10.1038/nclimate1546 (2012).

14 Mohseni, O., Stefan, H. G. & Erickson, T. R. A nonlinear regression model for weekly stream temperatures. *Water Resources Research* **34**, 2685-2692 (1998).

15 van Vliet, M. T. H. *et al.* Global River Discharge and Water Temperature under Climate Change. *Global Environmental Change* **23**, 450–464, doi:10.1016/j.gloenvcha.2012.11.002 (2013).

16 Koch, H. & Vögele, S. Dynamic modelling of water demand, water availability and adaptation strategies for power plants to global change. *Ecological Economics* **68**, 2031-2039 (2009).

17 UDI. World electric power plants database. (Utility Data Institute, Platts Energy InfoStore, available at http://www.platts.com/ (2013).

18 CARMA. Carbon Monitoring for Action database, available at http://carma.org/ (accessed 2014).

19 SEDAC. Socioeconomic Data and Applications Center, available at http://sedac.ciesin.columbia.edu/data/set/grump-v1-settlement-points (accessed 2014).

20 EIA. *U.S. Energy Information Administration, Independent Statistics & Analysis, International Energy Statistics*, http://www.eia.gov/ (accessed 2015).

21 Lehner, B. *et al.* High-resolution mapping of the world's reservoirs and dams for sustainable river-flow management. *Frontiers in Ecology and the Environment* **9**, 494-502, doi:10.1890/100125 (2011).

22 USGS. *GTOPO30 HYDRO1k elevation derivative database*, https://lta.cr.usgs.gov/HYDRO1K (accessed 2014).

23 NETL. National Energy Technology Laboratory Coal Power Plant Database (NETL-CPPDB) Available at http://www.netl.doe.gov/about/index.html (2007).

24 Weedon, G. P. *et al.* The WFDEI meteorological forcing data set: WATCH Forcing Data methodology applied to ERA-Interim reanalysis data. *Water Resources Research* **50**, doi:10.1002/2014wr015638 (2014).

25 GRDC, Global Runoff Data Centre, http://www.bafg.de/GRDC (D-56002 Koblenz, Germany) (accessed 2013).

26 GEMS/Water. Global Environment Monitoring System, http://www.gemstat.org/ (accessed 2015).

27 Hempel, S., Frieler, K., Warszawski, L., Schewe, J. & Piontek, F. A trend-preserving bias correction: the ISI-MIP approach. *Earth Syst. Dynam.* **4**, 219-236, doi:10.5194/esd-4-219-2013 (2013).

28 van Vuuren, D. P. *et al.* RCP2.6: exploring the possibility to keep global mean temperature increase below 2 degrees C. *Climatic Change* **109**, 95-116, doi:10.1007/s10584-011-0152-3 (2011).

29 Riahi, K. *et al.* RCP 8.5—A scenario of comparatively high greenhouse gas emissions. **109**, 33-57, doi:10.1007/s10584-011-0149-y (2011).

30 van Vuuren, D. P. *et al.* The representative concentration pathways: an overview. *Climatic Change* **109**, 5-31, doi:10.1007/s10584-011-0148-z (2011).

31 Craig, J., Landy, M., Conchie, S. & Sang, B. Small-scale hydropower: A methodology to estimate Europe’s environmentally compatible potential. 54 (The European Topic Centre on Air and Climate Change (ETC/ACC), Bilthoven, The Netherlands, 2010).

32 Eurelectric. Efficiency in electricity generation. Report No. Ref. 2003 – 030 - 0548, 30 (EURELECTRIC Preservation of Resources Working Group’s Upstream Sub-Group in collaboration with VGB, 2003).

33 Davies, E. G. R., Kyle, P. & Edmonds, J. A. An integrated assessment of global and regional water demands for electricity generation to 2095. *Advances in Water Resources* **52**, 296–313 (2013).

34 Koch, H., Vögele, S., Kaltofen, M. & Grünewald, U. Trends in water demand and water availability for power plants—scenario analyses for the German capital Berlin. *Climatic Change* **110**, 879–899, doi:10.1007/s10584-011-0110-0 (2012).

35 Yuan, Z. & Tol, R. S. J. Evaluating the costs of desalination and water transport. (Research unit Sustainability and Global Change, Hamburg University, Hamburg, 2004).

36 World Nuclear Association, http://www.world-nuclear.org/info/Current-and-Future-Generation/Cooling-Power-Plants/ (accessed 2015).

37 Stillwell , A. S. & Webber, M. E. Novel methodology for evaluating economic feasibility of low-water cooling technology retrofits at power plants. *Water Policy* **15**, 292–308 (2013).

38 Portmann, F. T., Döll, P., Eisner, S. & Flörke, M. Impact of climate change on renewable groundwater resources: assessing the benefits of avoided greenhouse gas emissions using selected CMIP5 climate projections. *Environmental Research Letters* **8**, 024023 (2013).

39 Moss, R. H. *et al.* The next generation of scenarios for climate change research and assessment. *Nature* **463**, 747-756, doi:10.1038/nature08823 (2010).